Redox-Dependent Structure Change and Hyperfine Nuclear Magnetic Resonance Shifts in Cytochrome $c^\dagger$

Yiqing Feng,[‡] Heinrich Roder, and S. Walter Englander*

Department of Biochemistry and Biophysics, University of Pennsylvania, Philadelphia, Pennsylvania 19104-6059

Received September 12, 1989; Revised Manuscript Received November 20, 1989

ABSTRACT: Proton nuclear magnetic resonance assignments for reduced and oxidized equine cytochrome c show that many individual protons exhibit different chemical shifts in the two protein forms, reflecting diamagnetic shift effects due to structure change, and in addition contact and pseudocontact shifts that occur only in the paramagnetic oxidized form. To evaluate the chemical shift differences ($\Delta\delta$) for structure change, we removed the pseudocontact shift contribution by a calculation based on knowledge of the electron spin g tensor. The g-tensor parameters were determined from the $\Delta\delta$ values of a large set (64) of $C_\alpha H$ protons at well-defined spatial positions in the oxidized horse protein. The g-tensor calculation, when repeated using only 12 available $C_\alpha H$ proton resonances for cytochrome c from tuna, proved to be remarkably stable. The largest principal value of the g tensor (g_z) falls precisely along the ligand bond between the heme iron and methionine-80 sulfur, while g_x and g_y closely match the natural heme axes defined by the pyrrole nitrogens. The derived g tensor was then used together with spatial coordinates for the oxidized form to calculate the pseudocontact shift contribution (Δpc) to proton resonances at 400 identifiable sites throughout the protein, so that the redox-dependent chemical shift discrepancy, $\Delta\delta - \Delta$pc, could be evaluated. Large residual changes in chemical shift define the Fermi contact shifts, which are found as expected to be limited to the immediate covalent structure of the heme and its ligands and to be asymmetrically distributed over the heme. Smaller chemical shift discrepancies point to a concerted change, involving residues 39–43 and 50–60 (bottom of the protein), and to other changes in the immediate vicinity of the heme ligands. Also, the three internal water molecules are implicated in redox sensitivity. The residues found to change are in good but not perfect agreement with prior X-ray diffraction observations of subangstrom redox-related displacements in the tuna protein. The chemical shift discrepancies observed appear in the main to reflect structure-dependent diamagnetic shifts rather than hyperfine effects due to displacements in the pseudocontact shift field. Although 51 protons in 29 different residues exhibit significant chemical shift changes, the general impression is one of small structural adjustments to redox-dependent strain rather than sizeable structural displacements or rearrangements.

Many studies directed at understanding the structure–function problem in cytochrome c have revealed that *ferri*cytochrome c is different from *ferro*cytochrome c in several physical and chemical properties, including global stability (Butt & Keilin, 1962), compressibility [Eden et al., 1982; see also Kharakoz and Mkhitaryan (1986)], molecular extent measured by low-angle X-ray scattering (Trewhella et al., 1988), hydrogen-exchange behavior (Ulmer & Kägi, 1968; Patel & Canuel, 1976; Wand et al., 1986; Liu et al., 1989), and the chemical reactivity of specific groups [e.g., Osheroff et al. (1980) and Arean et al. (1988)]. One may suspect a structural basis for these differences, but surprisingly small differences between *ferro*- and *ferri*cytochrome c are found in crystallographic studies of the tuna (Takano & Dickerson, 1981a,b) and yeast (A. Berghius and G. Brayer, personal communication) proteins at high salt concentrations and in a study of the coordination geometry of the heme by extended X-ray absorption fine structure spectroscopy (Labhardt & Yuen, 1979). Are the structures of oxidized and reduced cytochrome c in fact so similar under normal experimental conditions? Recent progress in solution NMR studies now permits investigation of this question.

Given NMR assignments for both *ferro*cytochrome c (Wand et al., 1989) and *ferri*cytochrome c (Feng et al., 1989), one way to proceed is to compare both structures in the solution state by use of two-dimensional nuclear Overhauser effect spectroscopy and distance geometry methods. Such studies of cytochrome c are in progress (A. J. Wand and M. Dellwo, personal communication). An alternative approach, pioneered by R. J. P. Williams and co-workers, is possible for proteins carrying a paramagnetic center [Williams et al., 1985b; see also Keller and Wüthrich (1972, 1978) and Lee et al. (1979, 1983)]. The presence of a single, fixed, highly anisotropic, and rapidly relaxing paramagnetic iron in oxidized cytochrome c produces resonance shifts of protons throughout the protein that depend on the position in space of each proton relative to the heme iron. Given the crystallographic structure of the oxidized protein and its electronic g tensor, the pseudocontact shift expected at the position of each proton can be computed. Protons on segments that are structurally displaced in the oxidized solution structure relative to the oxidized crystal structure should exhibit chemical shift increments (measured between oxidized and reduced solution forms) different from the paramagnetic shifts calculated by using the oxidized crystal structure. In their earlier work, Williams et al. (1985b) emphasized the use of this approach to search for structural differences between solution and crystal structures for oxidized tuna cytochrome c. At that time, only a relatively limited number of proton resonance assignments, cross assigned in tuna

ferri- and *ferro*cytochrome *c*, were available, and these were largely side-chain protons (Moore et al., 1985; Williams et al. 1985a).

The nearly complete proton resonance assignments of horse cytochrome *c* in both oxidation states (Wand et al., 1989; Feng et al., 1989) now allow a more detailed analysis. The newly available main-chain resonances were used here rather than the side-chain resonances utilized by Williams et al. (1985b), since main-chain protons can often be more precisely placed in the structure. A different approach was used for the data analysis, and the approach was broadened to distinguish crystal vs solution differences from oxidized vs reduced structure differences in solution. The results show that the overall structure of horse cytochrome *c* is extensively similar in the three forms just named but that significant structurally based chemical shift differences do occur between the oxidized and reduced proteins in solution. In addition, the analysis described yields a refined measurement of the electron spin *g* tensor and the heme Fermi contact shifts and thus provides further insight into the electronic structure of the ferric heme at room temperature.

Method of Analysis

While *ferro*cytochrome *c* is diamagnetic ($S = 0$), *ferri*-cytochrome *c* is paramagnetic ($S = \frac{1}{2}$), with an unpaired electron largely localized on the heme iron. The paramagnetic center adds hyperfine shifts, that is, contact and pseudocontact shifts, to the resonance frequency of many protons in the oxidized protein. For any given proton, the observed redox-dependent change in chemical shift, Δobs, can be represented as

$$\Delta obs = \delta_{ox} - \delta_{red} = \Delta c + \Delta pc,x + \Delta s \qquad (1)$$

where δ_{ox} and δ_{red} are the measured chemical shifts in the two different protein forms.

Δc represents the chemical shift increment due to Fermi contact interaction between a nuclear spin and the unpaired electron spin. It is commonly assumed that Fermi contact shifts are limited to protons on the heme and its immediate ligands as a result of the rapid attenuation of through-bond interactions with increasing number of intervening bonds (Wüthrich, 1976; Jardetzky & Roberts, 1981). If so, and results discussed below document this conclusion, then the great majority of protons, namely, those not associated with the heme, sense only the pseudocontact and structure terms.

$\Delta pc,x$ is defined here as the through-space pseudocontact contribution to proton chemical shifts, calculated for each proton at its spatial position in the oxidized crystal structure. Δs includes other chemical shift effects resulting from structure differences. Later we will separate the structure change term, Δs, into chemical shift effects due to structure differences between the oxidized crystal and solution forms ($\delta\Delta pc$), which are paramagnetic in origin, and diamagnetic effects (Δdi) due to differences between the two solution states (see eq 8c).

The approach used here attempts to define the positions of structure changes in cytochrome *c* by examining the chemical shifts of many protons throughout the protein in the reduced and oxidized solution states and determining those protons for which Δs is significantly different from zero. Because the pseudocontact shift contribution to Δobs can be calculated from the position of each proton relative to the unpaired heme electron, Δs can be obtained, for all protons but those on the heme and its ligands, as the measured Δobs minus the computed pseudocontact shift term, $\Delta pc,x$. Significant values for Δs can then be taken to mark the positions of structure changes.
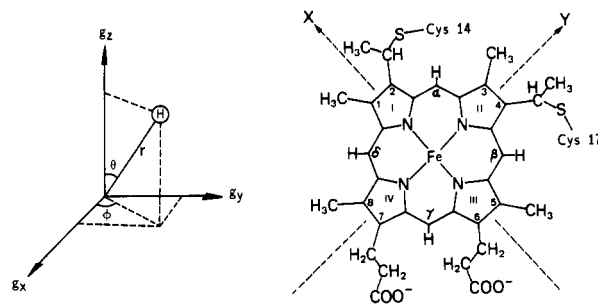

FIGURE 1: Nomenclature for positioning each proton in the *g*-tensor system (left) and for identifying heme-related groups (right). *X* and *Y* axes of the heme-based coordinate system are indicated; *Z* is normal to the heme plane. The pyrrole rings, viewed from Met-80, are numbered I–IV in a clockwise direction, and substituents at the eight pyrrole corners are numbered 1–8. The latter include ring methyls 1, 3, 5, and 8, propionates 6 and 7, and bridges 2 and 4 that join to the thioether linkages.

Since the calculation of the expected pseudocontact shifts uses the oxidized crystal structure coordinates, the approach is sensitive to structure changes among the three forms of cytochrome *c*, the oxidized crystal and solution structures and the reduced solution structure. This complexity is formalized and analyzed under Discussion.

g Tensor. Pseudocontact shifts are determined by the parameters of the electronic *g* tensor as follows (Kurland & McGarvey, 1970; Horrocks & Greenberg, 1973).

$$\Delta pc,x = [\beta^2 S(S + 1)/9kTr^3] \times$$
$$[g_{ax}(3\cos^2\theta - 1) + 1.5g_{eq}(\sin^2\theta\cos 2\phi)] \qquad (2a)$$

$$g_{ax} = g_z^2 - \tfrac{1}{2}(g_x^2 + g_y^2) \qquad (2b)$$

$$g_{eq} = g_x^2 - g_y^2 \qquad (2c)$$

Here β is the Bohr magneton, S is the electron spin quantum number ($\frac{1}{2}$ for ferricytochrome *c*), and T is absolute temperature. The position of each proton is defined by its polar coordinates (r, θ, ϕ) in the reference system of the electron spin *g* tensor (Figure 1A). The axial and equatorial anisotropies of the *g* tensor, g_{ax} and g_{eq}, are defined (eqs 2b and 2c) in terms of the principal components, g_i ($i = x, y, z$). Equation 2a assumes that the unpaired electron spin is effectively localized at the heme iron, which then acts as a point dipole.

The orientation of the *g*-tensor principal axis system relative to the heme coordinate system is usually defined by the three Euler angles, α, β, and γ. One starts with the g_x and g_y axes (Figure 1A) coincident with the heme *X* and *Y* axes (Figure 1B), and proceeds as follows: (i) rotate the g_xg_y plane through α about the heme *Z* axis; (ii) rotate the g_xg_y plane through β about the g_x axis obtained after (i); (iii) rotate the g_xg_y plane through γ about the g_z direction obtained after (ii). β defines the cone angle between g_z and the heme normal (and also the tilt of the g_xg_y plane out of the heme plane). α determines the rotational position of g_z in the cone, i.e., the direction of the projection of g_z onto the heme plane (at $\alpha + 90°$). When β is small, as found here, $\alpha + \gamma$ approximates the rotation of the orthogonal g_x and g_y axes relative to the heme *X* and *Y* axes (Figure 1B).

In their earlier work, Williams et al. (1985b) found the three separate g_i values by computing theory-based temperature-dependent corrections to the values measured by Mailer and Taylor (1972; by EPR at 4.2 K) and then fit the *g*-tensor angular parameters by considering the redox-dependent chemical shifts of 21 methyl group resonances. The much larger number of assigned proton resonances now available

(Wand et al., 1989; Feng et al., 1989) encouraged us to attempt to fit directly all five g-tensor parameters (g_{ax}, g_{eq}, α, β, γ). The agreement found between the two approaches is impressive (see Table I).

Least-Squares Fitting. To obtain the orientation and magnitude of the g tensor for oxidized cytochrome c, we relied on a large set of reference protons that experience neither significant contact shifts nor redox-dependent structure changes, i.e., protons for which Δc and $\Delta s \sim 0$, so that $\Delta pc,x = \Delta obs$ (eq 1). The best fit g-tensor parameters were found by minimizing the variance, χ^2 (eq 3), between the measured

$$\chi^2 = \sum(\Delta obs - \Delta pc,x)^2 \qquad (3)$$

(Δobs, eq 1) and calculated ($\Delta pc,x$, eq 2a) redox-dependent chemical shifts for the reference protons.

The refinement started with the g-tensor parameters found by Mailer and Taylor (1972) in EPR studies of cytochrome c crystals at 4.2 K ($\alpha = \beta = \gamma = 0°$; g_i values given in Table 1). The five parameters, α, β, γ, g_{ax}, and g_{eq}, were varied to obtain the optimal fit of $\Delta pc,x$ to Δobs for the protons in the reference set. To find the global minimum of χ^2 (eq 3), the three Euler angles were incremented independently in 20° steps over the range 0–360° for α, 0–180° for β, and 180–360° for γ. The optimal fit for g_{ax}, g_{eq}, and the Euler angles was searched for in the vicinity of each step by using a least-squares fitting algorithm.

The g tensor refined in this way could then be used to calculate $\Delta pc,x$ for all the other protons in oxidized cytochrome c. A comparison of the calculated $\Delta pc,x$ with the shift observed (Δobs) for each proton can then identify protons that do and do not experience significant resonance shifts due to structure change (Δs in eq 1).

Screen for Structure Change. To search for structure changes, we want to compare Δobs with $\Delta pc,x$ for many assigned protons throughout the protein and recognize the positions of significant discrepancies. However, the simple condition $|\Delta obs - \Delta pc,x| > 0$ is not a sufficient criterion for the presence of a structure change. The role of errors in measured proton chemical shifts, in proton positional coordinates, and in the calculation of $\Delta pc,x$ must also be considered.

Chemical shifts read from the spectra of reduced and oxidized proteins are accurate to within ±0.02 ppm, so that $\delta_{ox} - \delta_{red} = \Delta obs$ is known within ±0.04 ppm. The limited accuracy of the proton coordinates imposes an additional uncertainty on Δpc that we estimate as

$$|\delta\Delta pc| = \{|\partial\Delta pc/\partial r| + |\partial\Delta pc/r\partial\theta| + |\partial\Delta pc/r \sin\theta\partial\phi|\}\delta l \qquad (4)$$

Equation 4 relates the uncertainty in predicted chemical shift, $\delta\Delta pc$, to δl, the uncertainty in crystallographic coordinates, by scaling $\delta\Delta pc$ to the gradient of the pseudocontact shift field at the position of each proton. A small change, δl, in the coordinates of a proton can produce a small or large error in $\Delta pc,x$ depending upon the space gradient of Δpc at the proton position; this should be considered in judging the significance of an observed discrepancy. The use of the absolute value of each orthogonal component in eq 4 ensures that the maximum shift gradient is used for estimation of the error at each proton position. Thus, eq 4 estimates the positional uncertainty error, $\delta\Delta pc$, as the incremental pseudocontact shift that would result when the proton moves a total distance $1.7\delta l$, i.e., $(\delta l^2 + \delta l^2 + \delta l^2)^{1/2}$, along the direction of steepest pseudocontact shift gradient.

The protein was screened for structure changes at each proton position by looking for chemical shift discrepancies

between Δobs and $\Delta pc,x$ that are larger than the estimated maximum error level at that position, as in

$$|\Delta obs - \Delta pc,x| > \delta\Delta pc + 0.04 \qquad (5)$$

The size of the screen defined by eq 5 is set by the chemical shift uncertainty (0.04 ppm) plus $\delta\Delta pc$, determined by the positional uncertainty (eq 4). Because it is difficult to define a positional uncertainty from X-ray diffraction studies, the value used for δl in this study was not rigidly set; rather, δl was varied systematically over a reasonable range. As δl increases, the uncertainty estimate, $\delta\Delta pc$, increases, and fewer protons are caught in the screen. (The number of protons caught in the structure change screen defined by eq 5 is plotted as a function of δl in Figure 5.)

It can be noted that the screen is constructed to provide a stringent test for structure change by maximizing the estimated uncertainty level. In this work, we take $\delta l = 0.3$ Å, corresponding to a minimum displacement of 0.5 Å in the pseudocontact shift field, as the criterion for significant change. As a further protection against erroneous conclusions introduced by inaccuracies in the g tensor, Δpc was calculated for four additional g tensors having parameters varied in the vicinity of the refined g tensor (see last section under Results). An apparent discrepancy (eq 5) was accepted to signal structure change only when it was caught in all five tests. (Protons caught in all five screens are listed in Table III.)

In their earlier work, Williams and co-workers (1985b) more simply used a cutoff Δppm threshold as the criterion for evaluating structural change, namely, $|\Delta obs - \Delta pc,x| > 0.25$ ppm. We feel the present approach (eq 5) is an improvement since it evaluates possible discrepancies in terms of uncertainty in structure position and the sensitivity at each proton position to pseudocontact shift change (eq 4). Viewed conversely, eq 4 allows one to correlate a measured chemical shift discrepancy with the size of the structural displacement necessary to produce it. $\delta\Delta pc$ can be viewed in these two different ways, as an uncertainty in the calculated value of $\Delta pc,x$ due to uncertainty, δl, in spatial position (X-ray) or as a real change in chemical shift (Δobs, maximum) due to a structural displacement between the *oxidized* crystal and solution forms.

Structural Coordinates and NMR Chemical Shifts. Proton NMR chemical shifts were taken from assignments for the reduced and oxidized solution forms of horse cytochrome c at 20 °C (Wand et al., 1989; Feng et al., 1989), measured at pH 5.7 in phosphate buffer. Unpublished X-ray crystallographic results for oxidized horse cytochrome c at 1.9-Å resolution with an R factor of 0.172 were kindly provided by G. Bushnell, G. Louie, and G. Brayer. A number of proton NMR assignments are available for the tuna protein (Moore et al., 1985; Williams et al., 1985a). Coordinates for tuna *ferri*cytochrome c (both the inner and outer molecule of the crystalline unit cell) and *ferro*cytochrome c (Takano & Dickerson, 1981a,b) were obtained from the Brookhaven data bank.

Proton coordinates were generated from heavy atom coordinates by using the BIOGRAF molecular graphics program (BioDesign Inc., Pasadena, CA) with the usual assumption of standard amino acid geometries. Crystal structure coordinates, defined with respect to the unit cell, were transformed to a heme-based reference system with the X axis along the porphyrin N_1–N_3 direction, the Y axis along the N_2–N_4 direction, and the Z axis normal to these two vectors (Figure 1B). This is the orientation of the g tensor found in EPR studies of crystalline oxidized horse cytochrome c at 4.2 K (Mailer & Taylor, 1972). The angle between the N_1–N_3 and N_2–N_4 vectors is found to lie at 94° rather than 90°, and these

Table I: Heme Electronic g-Tensor Parameters for Oxidized Cytochrome c

source	principal axes			anisotropy factors		orientation			χ^2/N^d
	g_x	g_y	g_z	g_{ax}	g_{eq}	α	β	γ	
EPR[a]	1.25	2.25	3.06			~0	~0	~0	
prior work[b] (21 CH$_3$)	1.95	2.59	3.24			129	11	229	0.052
this work[c]									
horse (80 C$_\alpha$H)				4.92	−1.79	104	14	249	0.017
horse (64 C$_\alpha$H)	2.25	2.59	3.32	5.15	−1.65	106	13	251	0.004
tuna (12 C$_\alpha$H)									
inner				5.09	−2.32	99	14	246	0.003
outer				5.09	−2.12	108	13	248	0.004

[a] Measured by Mailer and Taylor (1972) in single crystals of horse cytochrome c at 4.2 K, with β to within ±3°, α and γ to ±5°. [b] Williams et al. (1985b) for tuna; g values calculated by using temperature dependence of electronic Zeeman effect and angular orientation from fitting of NMR data. [c] Computed for horse by using NMR data from Wand et al. (1989) and Feng et al. (1989) and X-ray results from Bushnell, Louie, and Brayer (personal communication); for tuna, NMR data from Williams et al. (1988) and X-ray data from Takano and Dickerson (1981a,b). [d] The statistical variance, with χ^2 defined as in eq 3.

two vectors are found not to be exactly coplanar (separation distance of 0.04 Å for horse, ~0.12 Å for tuna inner and outer). In all cases, the origin was placed at the midpoint of the four pyrrole nitrogens and a small adjustment was made to orthogonalize the two axes (X axis held constant). Refinement of the electron spin g tensor and calculations of pseudocontact shifts therefrom were performed on an IBM PC/AT computer using programs written with ASYST software (Asyst Software Technologies, Rochester, NY).

RESULTS

g Tensor for Horse Cytochrome c. The orientation and magnitude of the g tensor have been obtained by EPR measurements on single crystals of horse ferricytochrome c at 4.2 K by Mailer and Taylor (1972). However, in solution at 20 °C only the rotation-averaged magnetic susceptibility, which yields the rotation-averaged magnitude of the g tensor, has been measured (Angstrom et al., 1982). This is insufficient for the present analysis. The least-squares fitting procedure described before was performed to obtain the g tensor of horse *ferri*cytochrome c at room temperature.

At the first stage, a set of 80 C$_\alpha$ protons provided reference positions that represent the well-defined backbone structure of the protein. Of the 104 residues present, the C$_\alpha$H resonances not used are from the terminal residues 1–5 and 102–104, which are poorly defined in the crystallographic models, the heme ligand residues, which may have a significant contribution from Fermi contact shifts, and the glycine residues for which ambiguities exist due to the lack of stereospecific C$_\alpha$H resonance assignments. Side-chain protons and peptide group NH were not used in the reference set, because side chains tend to have more poorly defined positions and the chemical shifts of peptide NH are evidently very sensitive to small structural changes (see below). Given the initially refined g tensor, the screen for structure change was applied to the 80 reference C$_\alpha$ protons themselves by using the screening criterion of eq 5 and the $\delta\Delta$pc value for each proton obtained from eq 4 with $\delta l = 0.3$ Å. Of the 80 protons in the first-stage reference set, 16 show redox-dependent changes larger than allowed by the structure change screen.

A second-stage refinement was then performed by using as reference protons the subset of 64 C$_\alpha$H protons that passed the discrepancy screen. The 64 C$_\alpha$H used are from residues 7–13, 15, 19, 20, 22, 25–28, 30, 32, 33, 35, 36, 38–40, 43, 46, 47, 49, 50, 55, 58, 59, 61, 62, 64–70, 72, 73, 75, 76, 79, 81–83, 85–94, and 96–101. For this reference set, distances from the heme iron cover a range of 8–19 Å and the redox-dependent resonance shifts range from −1.1 to +2.0 ppm, with 33 of the 64 exhibiting absolute redox-dependent shifts larger than 0.30

ppm and 53 larger than 0.10 ppm.

Results are given in Table I. Though the variance is much improved in the second-stage refinement (Table I), the g-tensor parameters found do not differ significantly from the those of the first stage. The optimal fit was found for $\alpha = 106°$, $\beta = 13°$, and $\gamma = 251°$. Note that the sum, $\alpha + \gamma$, is close to 360°, so that the g_x and g_y axes of the g tensor in solution at 20 °C match the natural heme reference system, although the $g_x g_y$ plane is tilted out of the heme plane by 13° (apparently to make the Z axis congruent with the Met-80 S$_\delta$–Fe bond). The sensitivity of the refinement is illustrated in Figure 2, which compares the calculated Δpc with Δobs for different g-tensor parameter sets.

Figure 3 indicates how the rms deviation between observed and calculated paramagnetic shifts varies with the angular orientation of the g tensor. The angle β, which represents the tilt of the g_z axis away from the heme normal, is highly determined. The angle α, which determines the angular position of g_z within the cone defined by β, is less well determined than β by about 5-fold, matching their relative effect in displacing the course of the g_z vector through the Met-80 sulfur. For example, a change of 2.5° in β or of 12° in α is necessary to displace the g_z vector by 0.1 Å at the Met-80 sulfur (compare $r\,d\beta$ with $r\sin\beta\,d\alpha$, when $\beta = 13°$ so $\sin\beta = {}^1/_5$).

g Tensor for Tuna Cytochrome c. The g tensor in tuna *ferri*cytochrome c, previously computed by Williams et al. (1985b) using 21 assigned methyl groups as a reference set, was recalculated by the present method for the two crystallographically independent molecules (inner and outer) in the unit cell of the tuna *ferri*cytochrome c crystal, using as reference the reported redox-dependent shifts of 12 assigned C$_\alpha$ protons (Williams et al., 1985b; Arean et al., 1988; from residues 4, 11, 15, 19, 43, 51, 68, 78, 81, 83, 96, and 101). The parameters found, listed in Table I, are impressively similar to the horse protein g tensor refined with many more protons. The agreement found even with a small reference set speaks for the robustness of the g-tensor calculation.

Individual g Values at Different Temperatures. The magnitudes of the three principal g values cannot be individually determined by the present calculation alone (see eq 2a) but require a third constraint from an independent measurement, preferably at room temperature. The relationship in eq 6 connects magnetic susceptibility (χ) with g (Kurland &

$$\chi_i = N_A\beta^2 S(S + 1)g_i^2/3kT \qquad i = x, y, z \qquad (6)$$

McGarvey, 1970). The rotation-averaged magnetic susceptibility of horse *ferri*cytochrome c in solution was reported to be 30.5×10^{-6} M^{-1} (SI units) at 20 °C and pH 5.4, corresponding to an effective magnetic moment of 2.39 Bohr
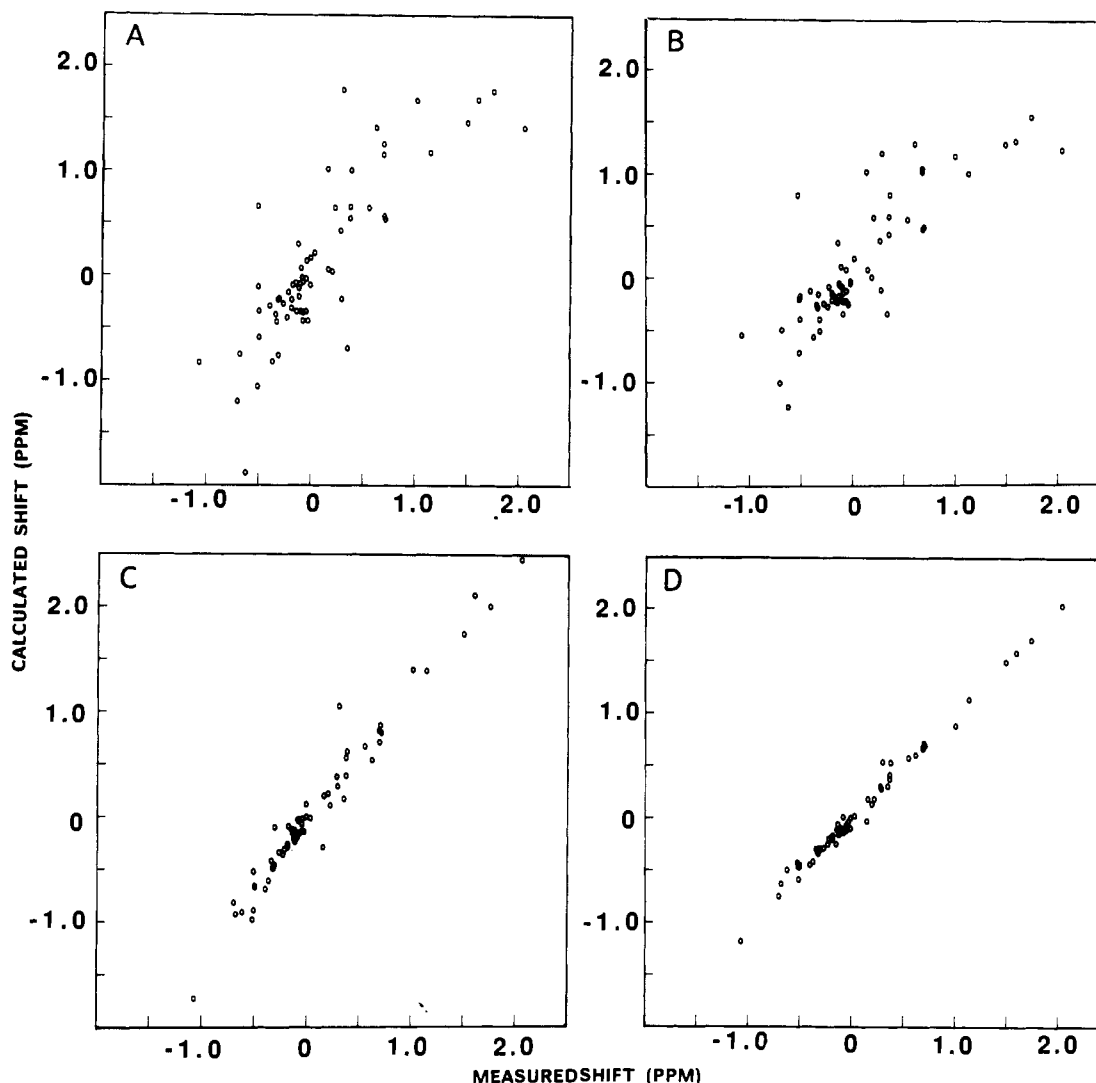
FIGURE 2: Comparison of computed and observed pseudocontact shifts for the 64 reference $C_\alpha H$ protons when different g-tensor parameters are used. (A) shows how Δobs values (measured redox-dependent shifts) for the reference protons differ from their calculated pseudocontact shifts when the g tensor has the Mailer and Taylor (1972) parameters (Table I). (B) was computed also for $\alpha = \beta = \gamma = 0°$ but with our best fit g_{ax} and g_{eq} values (Table I), while (C) shows the agreement with our best fit orientation and the 4.2 K g_i values. In (D), computed shifts are from the final best fit g tensor.

magnetons (Angstrom et al., 1982). With this value, eq 6 yields $(g_x^2 + g_y^2 + g_z^2)/3 = 7.62$. Given this result together with the g_{ax} and g_{eq} (eqs 2b and 2c) found in the refinement, the individual g values can be obtained. Table I compares the g values found in EPR studies of the crystalline horse protein at 4.2 K (Mailer & Taylor, 1972), the values computed by Williams et al. (1985b), who considered the temperature dependence of the Zeeman effect to extrapolate the EPR values to room temperature, and the values found in the present work.

Analysis of Redox-Dependent Chemical Shifts. The refined g tensor was used to calculate pseudocontact shifts at over 400 positions ($\sim$600 assigned protons) in horse *ferri*cytochrome *c*. (The more distal protons of the lysines and a few other residues were not available.) For methyl groups and fast-flipping aromatic rings having protons in fast stereochemical exchange, the pseudocontact shift for each proton was calculated separately and the average shift tabulated. For cases in which stereospecific resonance assignments are lacking, such as the geminal $C_\alpha H_2$ of glycines and $C_\beta H_2$ of methylene groups and for the paired methyl groups of valines and of leucines, a choice could often be made by matching Δobs values with the Δpc,x calculated for the two ambiguous protons (suggesting the stereospecific assignments in passing). Results are illustrated in Figure 4.

The list of protons was then screened for redox-dependent chemical shift changes that could not be explained by the pseudocontact contribution. The test for structure change defined in eq 5 was applied with δl (eq 4) taken as 0.3 Å (corresponding to a real space displacement of 0.3 Å $\times$ 1.7 = 0.5 Å in the direction of maximum shift gradient) to impose a small screen that would catch most protons that experience significant changes. However, to avoid overcapture due to inaccuracy in the g tensor, the test was repeated with four other g tensors having altered parameters, namely, with $\alpha = \alpha_0$, $\beta = \beta_0 \pm 2°$, $\gamma = \gamma_0$, and $\alpha = \alpha_0 \pm 15°$, $\beta = \beta_0$, $\gamma = \gamma_0 \mp 15°$. ($\alpha_0$, β_0, and γ_0 are the values listed in Table I for the horse second-stage refinement.) These latter tests used $|\delta \Delta pc'| = |\delta \Delta pc^0| + |\partial \Delta pc/\partial g_{ax}|\delta g_{ax} + |\partial \Delta pc/\partial g_{eq}|\delta g_{eq}$, with $|\delta \Delta pc^0|$ from eq 4, and $\delta g_{ax} = \delta g_{eq} = 0.2$.

Protons that show chemical shift discrepancies for all five g tensors are listed in Tables II and III. The protons in Table II are discussed below in terms of Fermi contact shifts. The discrepant protons listed in Table III experience structure change (see also Figure 4). Figure 5 shows the number of protons caught as the screen is tightened (δl decreased). When δl is set in the range of 2 Å so that only highly discrepant resonance shifts are caught by the screen, most of the protons found are in two neighboring segments, between residues 39–43
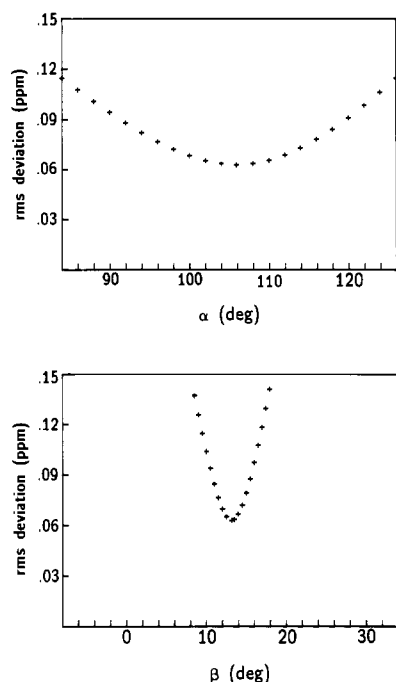
FIGURE 3: Sensitivity of the calculation for angular parameters of the g tensor. The plots show the root mean square deviation of chemical shift discrepancy, $[\sum(\Delta obs - \Delta pc,x)^2/(N - 1)]^{1/2}$, for the 64 $C_\alpha H$ reference protons as the g-tensor angles are varied. In the top panel, β is kept at 13° while α is varied about its best fit value of 106° and γ is varied in a complementary way to hold $\alpha + \gamma$ constant at 357°. Here the Z axis is rotated around the conical surface defined by $\beta = 13°$ while the $g_x g_y$ orientation in the heme system is held constant. In the bottom panel, the tilt angle β is varied while the best fit values of α and γ (Table I) are held constant.

and 50–60 (see Figure 6). When the screen is made tighter, with δl decreasing to 0.3 Å (corresponding to an 0.5-Å discrepancy in real space), the protons listed in Table III are caught. When the screen is decreased below $\delta l = 0.3$ Å, one sees the *onset* of extensive proton capture (Figure 5). This appears to relate to the noise level of the X-ray determination and/or the error level in the pseudocontact shift calculation (the *mean* noise level is much below $\delta l = 0.3$ Å).

A table for all the NH, $C_\alpha H$, and $C_\beta H$ protons and many of the side-chain protons in cytochrome c, listing Δobs, $\Delta pc,x$, $\Delta obs - \Delta pc,x$, and $\delta \Delta pc$ calculated by using the best fit g-tensor parameters and $\delta l = 0.3$ Å, can be found in the dissertation of Y. Feng (1989) and is available on request.

Electron Spin Delocalization. The problem of electron spin delocalization onto the porphyrin ring and axial ligands has received considerable attention in terms of the degree of delocalization and chemical shift effects to be expected (Kurland & McGarvey, 1970; Shulman et al., 1971; Horrocks & Greenberg, 1973; Wüthrich & Baumann, 1974; LaMar & Walker, 1979). In the present work, observed chemical shifts were used to fit the parameters of eq 2a, and the equation obtained was then used to predict the pseudocontact shift contribution to many protons throughout oxidized cytochrome c. Widespread agreement between calculated and observed shifts was obtained. At this level, it can be said that eq 2a can accurately describe the pseudocontact shift field. To deal specifically with the issues raised in the work cited just above, a deeper analysis may well be necessary.

DISCUSSION

In this work the paramagnetic g tensor of the oxidized heme in cytochrome c was calculated from measured chemical shift differences between oxidized and reduced cytochrome c by

Table II: Contact Shifts for Oxidized Horse Cytochrome c

protons	pyrrole	Δobs^a	$\Delta pc,x^b$	Δc ($\Delta obs - \Delta pc,x$)	$\delta \Delta pc^c$ ($\delta l = 0.1$ Å)
meso CH					
β	II–III	−10.4	−5.2	−5.2	1.05
γ	III–IV	−1.6	−8.5	6.9	1.14
ring methyls					
1	I	3.3	−4.3	7.6	0.36
3	II	29.2	−2.4	31.6	0.36
5	III	6.1	−5.2	11.3	0.20
8	IV	33.7	−2.7	36.4	0.22
Cys-14	I				
$C_\alpha H$		−0.9	−0.5	−0.4	0.29
$C_\beta H/C_\beta H'$		0.6	0.7/1.1	−0.1/0.5	0.16/0.44
bridge 2 CH		−6.5	−5.4	−1.1	0.50
bridge 2 CH$_3$		−4.1	−3.7	−0.4	0.20
Cys-17	II				
$C_\alpha H$		1.9	0.9	1.0	0.16
$C_\beta H/C_\beta H'$		5.6	0.6/−1.5	5.0/7.1	0.65/0.36
bridge 4 CH		−4.2	−4.3	0.1	0.32
bridge 4 CH$_3$		0.6	−1.3	1.9	0.10
propionate 6	III				
$C_\alpha H/C_\alpha H'$		−5.7	−5.0/−3.2	−0.7/−2.5	0.37/0.47
propionate 7	IV				
$C_\alpha H$		15.7	−1.6	17.3	0.13
$C_\alpha H'$		7.4	−1.5	8.9	0.27
His-18					
$C_\alpha H$		5.4	5.1	0.3	0.31
$C_\beta H$		8.2	7.4/8.1	0.8/0.1	0.40
$C_\beta H'$		13.7	7.4/8.1	5.6/6.3	0.64
$N_\pi H$		3.2	9.6	−6.4	0.82
C_2H^d		−26.1	11.6	−37.7	3.3
C_5H^d		24.9	38.9	−14.0	5.8
Met-80					
$C_\alpha H$		−0.2	0.8	−1.0	0.62
$C_\beta H/C_\beta H'$		13.0	12.4/10.5	0.6/2.5	2.2/0.9
$C_\gamma H/C_\gamma H'$		−25.0	16.8/15.9	−41.8/−40.9	1.5/2.8
$C_\epsilon H_3$		−21.6	11.7	−33.3	2.6

[a] Redox-dependent chemical shift difference, obtained as $\Delta obs = \delta_{ox} - \delta_{red}$, in parts per million at 20 °C, pH 5.7. [b] Pseudocontact shift, calculated by using the second-stage-refined g tensor (Table I). [c] The calculated change (eq 4) in pseudocontact shift due to a displacement of 1.7×0.1 Å in the direction of maximum gradient. [d] Current IUPAC nomenclature, corresponding to prior C_2H and C_4H, respectively.

using a large number of $C_\alpha H$ protons at well-defined spatial positions. The g tensor was then used to estimate pseudocontact shifts at many proton positions throughout the protein. Here we consider the orientation of the g tensor itself and implications of the discrepancies found between the pseudocontact shifts computed from it and the redox-dependent chemical shifts actually observed.

g Tensor and the Sulfur Ligand. The results obtained here show that, for oxidized cytochrome c in solution at room temperature, two of the principal axes of the g tensor, the g_x and g_y axes, are only minimally offset from the heme N_1–N_3 and N_2–N_4 vectors, while the g_z axis is significantly tilted away from the heme normal. The g_z axis falls accurately along the Fe–S ligand bond, passing through the sulfur atom at 0.07 Å from its apparent center of mass. Essentially, the same g-tensor orientation was found for both horse and tuna cytochromes c. The g values found are close to those calculated by Williams et al. (1982b) using first- and second-order Zeeman corrections, indicating the importance of the latter contribution (Horrocks & Greenberg, 1973).

Earlier work on a series of cytochromes c has dealt with the effects of heme ligands on the electronic structure of the heme
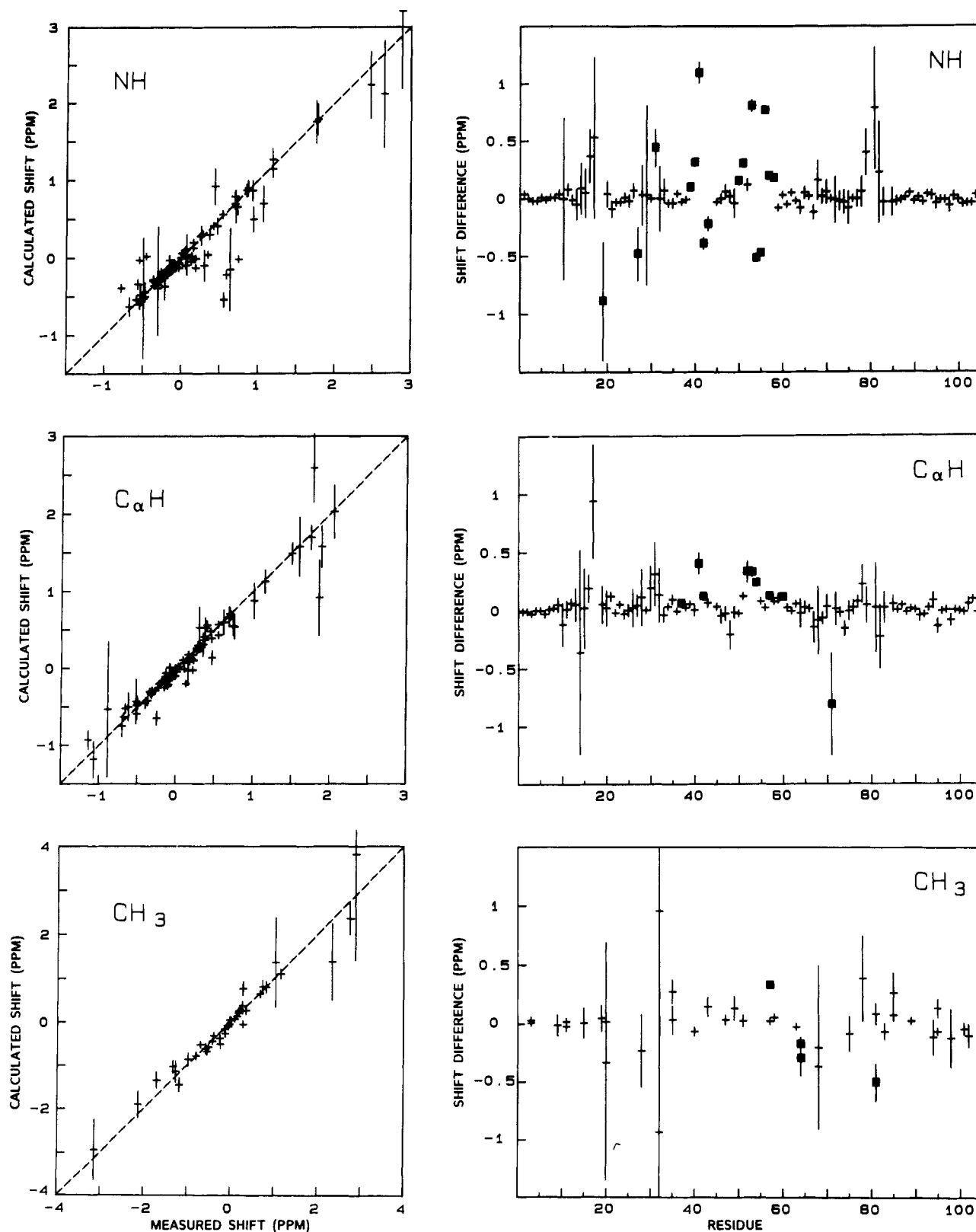
FIGURE 4: Comparison of measured redox-dependent shifts and calculated pseudocontact shifts for NH, $C_\alpha H$, and CH_3 groups in horse ferricytochrome c (excluding Cys-14 and -17, His-18, and Met-80). On the left, the calculated pseudocontact shifts ($\Delta pc,x$, eq 2a) are plotted against the measured shifts (Δobs, eq 1). On the right, the shift difference ($\Delta obs - \Delta pc,x$) is plotted against residue number. Vertical bars represent the computed shift uncertainty, $\pm\delta\Delta pc$, from eq 4 with $\delta l = 0.3$ Å. Solid squares indicate protons caught by the structure change screen when $\delta l = 0.3$ Å (listed in Table III).

[Redfield & Gupta, 1971; Keller & Wüthrich, 1978; reviewed by Satterlee (1986)]. Studies using NMR spectroscopy and circular dichroism have indicated that the electronic structure of the heme is strongly affected by the coordination of the axial methionine; in different cytochrome c species, rotation of the

in-plane g-tensor axes (Senn et al., 1980) and apparent asymmetry of the unpaired electron spin density over the heme plane (Senn et al., 1983) were observed to follow changes in the orientation of the methionine ligand even though the axial histidine ring orientation remained unchanged. The result

Table III: Protons That Show Significant Discrepancies between Δobs and Δpc,x[a]

proton	Δobs[b]	Δpc,x[c]	Δobs − Δpc,x	δΔpc[d] (δl = 0.3 Å)	δl_crit[e] (Å)
T19[f] NH	2.88	3.77	−0.89	0.51	0.5
K27[f] NH	0.44	0.92	0.48	0.23	0.6
P30 $C_\beta H$	0.12	−0.38	0.50	0.20	0.7
N31[f] NH	0.94	0.50	0.44	0.16	0.7
H33[f] $C_2 H$	0.37	0.14	0.23	0.01	5.7
G37 $C_\alpha H$	0.00	−0.09	−0.09	0.01	1.5
K39[f] NH	−0.03	−0.13	0.10	0.01	1.8
T40[f] NH	0.19	−0.13	0.32	0.02	4.2
G41[f] NH	0.56	−0.54	1.10	0.09	3.5
$C_\alpha H_2$	−0.25	−0.65	−0.40	0.09	1.2
	−0.22	−0.45	0.23	0.06	1.0
Q42[f] NH	−0.78	−0.39	−0.39	0.05	2.1
$C_\alpha H$	−0.11	−0.23	0.12	0.02	1.2
A43[f] NH	−0.56	−0.34	−0.22	0.06	0.9
D50[f] NH	0.06	−0.10	0.16	0.03	1.2
A51[f] NH	0.35	0.04	0.31	0.03	2.7
$C_\alpha H$	0.23	0.11	0.12	0.03	0.8
N52[f] $C_\alpha H$	0.47	0.14	0.33	0.09	1.0
$C_\beta H_2$	0.13	−0.18	0.31	0.13	0.6
	0.10	−0.40	0.50	0.11	1.2
K53[f] NH	0.59	−0.22	0.81	0.05	4.6
$C_\alpha H$	0.13	−0.20	0.33	0.04	2.2
$C_\beta H_2$	(−0.03)	−0.16	0.13	0.03	0.9
	(−0.03)	−0.13	0.10	0.02	0.9
N54[f] NH	−0.54	−0.03	−0.51	0.02	7.1
$C_\alpha H$	0.22	−0.02	0.24	0.01	6.0
$C_\beta H$	0.18	0.03	0.15	0.01	3.3
K55[f] NH	−0.45	0.02	−0.47	0.02	6.5
G56[f] NH	0.75	−0.02	0.77	0.02	11.0
I57[f] NH	0.19	−0.01	0.20	0.01	4.8
$C_\alpha H$	0.11	−0.01	0.12	0.01	2.4
$C_\gamma H_2$	0.29	0.10	0.19	0.03	1.5
	0.24	0.00	0.24	0.02	3.0
$C_\delta H_3$	0.29	−0.05	0.34	0.03	3.0
T58 NH	0.13	−0.05	0.18	0.01	4.2
$C_\beta H$	0.01	−0.08	0.09	0.01	1.5
W59[f] $C_2 H$	−0.12	−0.43	0.31	0.04	2.0
$C_7 H$	0.57	0.11	0.46	0.15	0.8
K60 $C_\alpha H$	−0.10	−0.21	0.11	0.02	1.1
L64 $C_\delta H_3$	0.69	−0.52	−0.17	0.06	0.7
	−1.32	−1.03	−0.29	0.15	0.5
E66 $C_\beta H_2$	0.20	0.01	0.19	0.02	2.2
	0.23	0.07	0.16	0.03	0.8
Y67[f] $C_\beta H$	−0.06	0.28	0.34	0.11	0.9
OH	12.69	6.58	6.11	2.06	0.9
L68 $C_\delta H_3$	−1.70	−1.34	−0.36	0.18	0.5
P71 $C_\alpha H$	1.78	2.59	−0.81	0.44	0.5
$C_\beta H$	4.86	6.65	−1.79	1.29	0.4
K72 $C_\beta H_2$	1.13	0.92	0.21	0.08	0.6
	1.12	0.92	0.20	0.08	0.6
I81 $C_\delta H_3$	0.28	0.78	−0.50	0.16	0.9

[a] Protons listed are caught in the structure change screen (eq 5) for all five g-tensor parameter sets used when δl is set at 0.3 Å. The $\delta l = 0.3$ Å criterion sets the base line for changes recognized to be significant as the chemical shift that would be obtained for a movement in the paramagnetic shift field ≥ 0.5 Å. [b] Chemical shift difference, obtained as Δobs = $\delta_{ox} - \delta_{red}$, in parts per million measured at pH 5.7, 20 °C. Parentheses indicate that, in one of the oxidation states, only one proton of the geminal pair is assigned. [c] Pseudocontact shift calculated for oxidized horse cytochrome c X-ray coordinates (Bushnell, Louie, and Brayer, personal communication) by using the second-stage-refined g tensor (Table I). [d] The maximum pseudocontact shift field gradient at the proton position, expressed in parts per million per 0.3 Å, calculated from eq 4 and the second-stage-refined g-tensor parameters (Table I). [e] The minimum movement (in angstroms) within the pseudocontact shift field necessary to produce the observed chemical shift discrepancy (Δobs) is given by $1.7\delta l_{crit}$ (see eq 4). The calculation for δl_{crit}, used only the first derivative of the pseudocontact shift field, thus will be inaccurate for large calculated displacements. [f] Residues found to experience redox-dependent displacement in the X-ray study of tuna cytochrome c (Takano & Dickerson, 1981a,b). Additional residues noted to experience change in the X-ray work are as follows: (a) in the His-18 region, Val-28, Gly-29, Leu-32, which together with the residues implicated here fill in the continuous sequence from Lys-27 to His-33; (b) in the middle region, Arg-38, Thr-47, and "slight" movements in Y48, T49, which tend to fill in the bottom of the protein, from Gly-37 to Ala-43 and from Tyr-48 to Lys-60; (c) near Met-80, Phe-82 and Ala-83; (d) heme-associated residues, Cys-17, His-18, Met-80, which were specifically excluded from this table (see Table II).
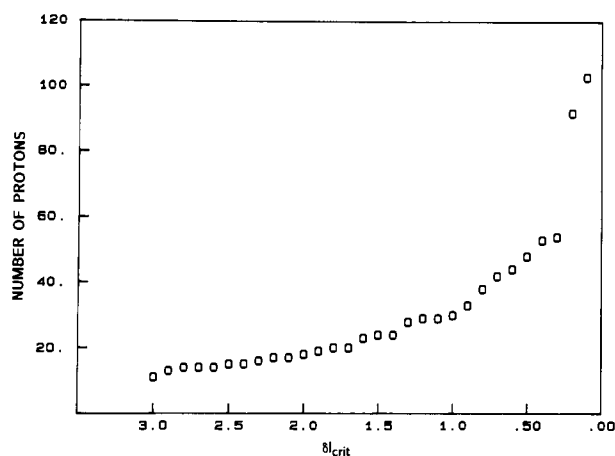

FIGURE 5: Number of protons caught by the discrepancy screen (eq 5), using the best fit g tensor (Table I), as δl is decreased from large values.

obtained here also speaks for the role of the methionine ligation in setting the position of the electron orbital vacated in the heme oxidation process.

One can further consider the possible implications of these results for oxidation and reduction kinetics. Since little structure change occurs in the redox transition [see below and also Takano and Dickerson (1981a,b); A. Berghius and G. D. Brayer, personal communication; Labhardt & Yuen, 1979], it appears that the electron orbital occupied in the reduced state and vacated in the oxidation process may be oriented with the Fe–S bond in both states. It seems plausible that this situation is exploited by the protein to achieve the maximum electron-transfer rate.

Contact Shifts. Proton resonance assignments for the heme group and its covalently linked residues and ligands in reduced and oxidized horse cytochrome c have recently been completed (Santos & Turner, 1987; Feng et al., 1990). In the oxidized heme, the unpaired electron density causes a number of heme-related protons to exhibit large hyperfine shifts, reflecting scalar Fermi contact interactions due to proton–electron spin density overlap, in addition to the dipole–dipole pseudocontact shifts dealt with above. The present analysis for the pseudocontact shift contribution now allows the true contract shifts to be evaluated.

Table II provides a nearly complete accounting of redox-dependent shifts (Δobs) of the heme-related protons, and for each proton divides Δobs into the computed pseudocontact shift contribution (Δpc,x) and the increment not explained by the pseudocontact shift. The latter is evidently dominated by the Fermi contact shift (Δc), although any imperfection in the point dipole approximation (eq 2a) for calculating Δpc will be most pronounced here.

Unlike the relatively symmetric effects seen in model hemes (Wüthrich et al., 1969), the contact shifts around the heme reveal a highly asymmetric distribution of unpaired electron spin, as has been noted before (Redfield & Gupta, 1971; Keller & Wüthrich, 1978; Satterlee, 1986). Substituents on one
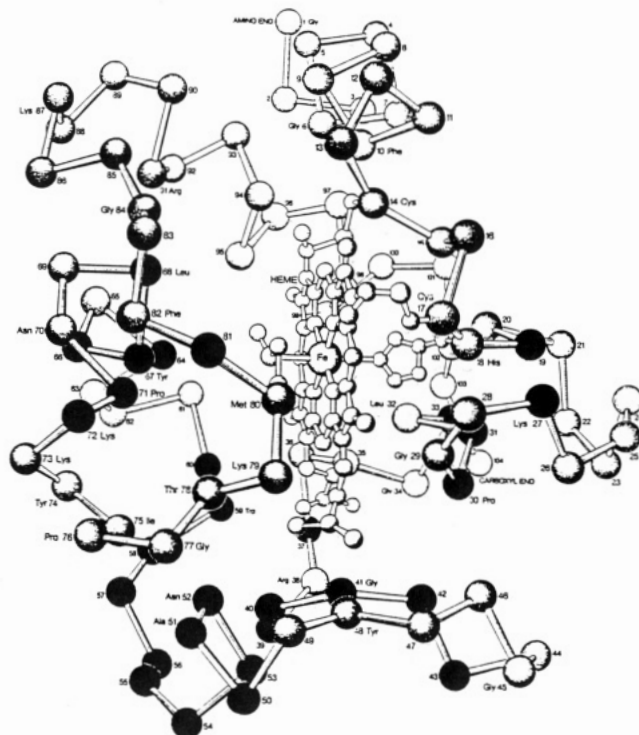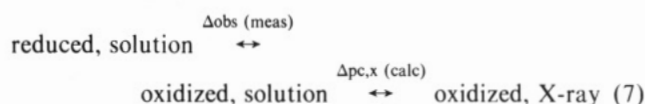
FIGURE 6: Skeletal α-carbon model of cytochrome c showing the residues (blackened) with protons that are caught in the screen for significant redox-dependent change in chemical shift.

diagonal (pyrroles II and IV) exhibit much larger downfield (positive) shifts than on the other (pyrroles I and III). Thus, large downfield shifts occur at the methyl groups on pyrroles II and IV, and lesser, although still large, shifts at the pyrrole I and III methyls. Also, the $C_\alpha H$ of propionate 7, on pyrrole IV, shows a much larger positive shift than the corresponding proton on pyrrole III. Protons on the two thioether bridges to pyrroles I and II exhibit generally small effects, but have opposite sign, as do also the β and γ meso protons (bridging between pyrroles II and III, and between III and IV, respectively). The meso proton shifts appear small, considering that they are bonded directly to the macrocycle; the α and δ meso proton resonances have not been found, possibly due to much larger contact effects at these positions.

The results in Table II document the rapid fall-off of the Fermi contact effect with number of intervening bonds. Unpaired electron spin density appears not to extend significantly into the Cys-14 and Cys-17 substituents or even their bridging groups, bonded directly to pyrroles I and II. Here the bond angle relative to the heme plane may play a role (Shulman et al., 1971). Among the iron ligands, the $C_\gamma H$ and $C_\epsilon H$ of Met-80, which are two bonds removed from the liganding sulfur, show large upfield (negative) shifts, while the $C_\beta H$, three bonds removed, is hardly shifted. Similarly in His-18, the $C_2 H$ and $C_5 H$ protons (IUPAC nomenclature, formerly $C_2 H$ and $C_4 H$), two bonds from the liganding nitrogen, are strongly upfield shifted while the $N_\pi H$, three bonds away, shows a much smaller effect. It can be noted that the anomalous shifts of the His-18 $C_2 H$ and $C_5 H$, which seem to have large and oppositely signed redox-dependent shifts, are rationalized by the pseudocontact shift calculation.

Test for Structure Change. Let us briefly review the logic of the search for structure change used here by reconsidering the terms in eq 1. From here on, we ignore the contact shift (Δc), which is localized to the heme and its ligands (Table II), and consider non-heme-associated changes, where $\Delta c = 0$ (Table III).

The analysis pursued here deals with chemical shift relationships between two pairs of forms, as diagrammed in eq 7, which indicates the source of the chemical shift parameters

$$\text{reduced, solution} \quad \overset{\Delta\text{obs (meas)}}{\longleftrightarrow}$$

$$\text{oxidized, solution} \quad \overset{\Delta\text{pc,x (calc)}}{\longleftrightarrow} \quad \text{oxidized, X-ray} \quad (7)$$

between each pair of structures considered, obtained either by NMR measurement (oxidized vs reduced solution structures) or by calculation (oxidized X-ray vs oxidized solution structures).

Conformational differences between the reduced and oxidized molecules in solution produce diamagnetically based chemical shift differences, Δdi, just as for any protein in two solution conformations. In addition, protons in oxidized cytochrome c in solution are subject to pseudocontact shifts, $\Delta\text{pc,s}$, which vary with their position in space relative to the paramagnetic center. Observed chemical shift differences (Δobs) between the two solution-state conformations thus include two components, as in eq 8a (for non-contact-shifted resonances).

$$\Delta\text{obs} = \Delta\text{di} + \Delta\text{pc,s} \quad (8a)$$

$$\Delta\text{pc,s} = \Delta\text{pc,x} + \delta\Delta\text{pc} \quad (8b)$$

$$\Delta\text{obs} - \Delta\text{pc,x} = \Delta\text{s} = \Delta\text{di} + \delta\Delta\text{pc} \quad (8c)$$

The pseudocontact shift contribution for each proton in the oxidized X-ray structure ($\Delta\text{pc,x}$) can be computed from its X-ray coordinates and the g tensor. If the oxidized X-ray and solution structures are identical, then $\Delta\text{pc,x} = \Delta\text{pc,s}$. However, these quantities will not be equal if the proton position in the oxidized solution structure is imperfectly represented by the X-ray model, due to errors in the model or to real structural differences between the crystal and solution states. To account for this discrepancy, $\Delta\text{pc,x}$ must be adjusted by the term $\delta\Delta\text{pc}$, as in eq 8b.

The available data for each proton are the measured chemical shift difference, Δobs, and the computed pseudocontact shift term, $\Delta\text{pc,x}$. We test for structure change by examining the chemical shift difference, $\Delta\text{obs} - \Delta\text{pc,x}$ (eq 8c). It can be seen that the difference found, equal to the structure change term, Δs (eqs 1 and 8c), may actually involve structure changes among the three protein forms. Δdi specifically derives from structural changes between the two solution forms, while $\delta\Delta\text{pc}$ specifically represents discrepancies between the oxidized crystal and solution forms (related to δl as in eq 4).

On the Analytical Method. In their initial exploration of the paramagnetic shift structure change analysis, Williams et al. (1985b) emphasized changes *between the solution and crystal structures* of cytochrome c and explicitly assumed that the two solution forms were identical, because the two crystal forms (Takano & Dickerson, 1981a,b) seemed so similar. This is equivalent to assuming that $\Delta\text{di} = 0$ so that $\Delta\text{obs} - \Delta\text{pc,x} = \delta\Delta\text{pc}$ (eq 8c). Results obtained here now appear to show that one cannot assume $\Delta\text{di} = 0$; rather, the size and distribution of the changes found indicates that Δdi can be a dominant factor (see below).

In the approach adopted by Williams et al. (1985b), the presence of structure change between the crystal and solution structures was inferred when the value found for $\Delta\text{obs} - \Delta\text{pc,x}$ was greater than 0.25 ppm. The present results indicate that this criterion can be misleading. Many of the protons that would appear to experience change when judged by the 0.25 ppm criterion are not caught in the screen we used, since they occupy a region of space with high shift gradient, and a

Table IV: Redox-Sensitive Protons and Internally Bonded Waters[a]

W1		W2		W3	
H bond	sensitive H	H bond	sensitive H	H bond	sensitive H
Asn-52 Nδ	Asn-52 C$_\alpha$H Asn-52 C$_\beta$H$_2$	Thr-19 NH	Thr-19 NH	Arg-38 Nϵ	
Tyr-67 O$_\eta$	Tyr-67 O$_\eta$H	Lys-25 CO		Lys-39 CO	Lys-39 NH Thr-40 NH
Thr-78 O$_\gamma$		Lys-27 NH	Lys-27 NH	Gln-42 NH	Gln-42 NH Gln-42 C$_\alpha$H
		Gly-29 CO			

[a] Groups found to be within H-bonding distance of each of the three internal water molecules (W1, W2, W3) in tuna cytochrome c (Takano & Dickerson, 1981a) are listed, along with redox-sensitive protons, from Table III, that may relate to these H bonds.

positional error smaller than 0.5 Å would produce the chemical shift discrepancy observed. In the other direction, half of the protons found by the present criteria to experience structure-related change in chemical shift (Table III) show discrepancies of less than 0.25 ppm. Many of these would have to move more than 1 Å in the pseudocontact shift field to account for the shift increment observed and thus are judged significant. As a result of these procedural differences, together with the fact that the resonance assignments of only a few of the protons in Table III were available to Williams and co-workers in 1985, the list of protons found to experience significant structure-dependent change in this work bears little resemblance to those found earlier in the initial development of this approach.

Changes Found. The significant chemical shift discrepancies found are listed in Table III. These are concentrated in limited regions of the protein, involving two connected sequences at positions in the low 40s and the 50s and also some discontinuous residues near both heme ligands (Figures 4 and 6). The large size and concerted nature of the chemical shift discrepancies point to a structural basis for these effects. Additional protons in some of the residues listed in Table III are caught in the structure-change screen but have small δl_{crit}, close to 0.3 Å, and are able to pass the screen in one or more of the five g-tensor tests imposed. The changes found by NMR are in good, although not perfect, agreement with the residues seen to change in the X-ray determination. Residues in Table III that were also noted by X-ray diffraction to experience small, subangstrom displacements (in the tuna protein; Takano & Dickerson, 1981a,b) are marked.

The NMR results obtained are correlated with the cytochrome c structure in Figure 6. The sensitive 50s segment lies between Tyr-48 and Trp-59, both of which H bond to the heme propionate 7 carboxyl oxygens. The segment consisting of residues 39–42 underlies propionate 7 and the plane of Trp-59, and the 50s segment arcs around it. These two segments are connected by several H bonds and form the "bottom" of the protein (Figure 6).

Among the six residues listed at the top of Table III, four are closely involved with the His-18 heme ligand (T19, K27, P30, N31). The His-18 ring N$_x$H is H bonded to the Pro-30 carbonyl, vicinal to the sensitive Asn-31 NH. The Thr-19 NH and Lys-27 NH are within H-bonding distance of an internal water molecule (W2 in Table IV) that is close to His-18 N$_\delta$. On the opposite heme face, the sensitive Tyr-67 OH (Table III) bonds directly to the Met-80 sulfur ligand. The sensitive side-chain methyls of Leu-64 and -68 form a complex that contacts the Tyr-67 and Trp-59 rings and the heme methyls 1 and 8. Also, the sensitive Pro-71 C$_\alpha$H and C$_\beta$H contact the Tyr-67 ring.

Takano and Dickerson (1981a) describe three internal water molecules in tuna cytochrome c, each one potentially H bonded to three or four amino acid residues. It is noteworthy that the

groups implicated in this way and/or their nearest-neighbor protons are heavily represented in the list (Table III) of redox-sensitive protons. These relationships are shown in Table IV.

In most residues caught in the structure-change screen (Table III), the peptide NH exhibits the largest chemical shift discrepancy. Evidently, the chemical shifts of peptide NH are particularly sensitive to small strains or distortions in the main chain, perhaps due to proximity to the peptide bond and/or to H bonding [see also Wagner et al. (1983)]. The main-chain NH dominate the changes in Table III about His-18 and in the 40s and 50s segments but are absent in the Met-80 ligand region.

In light of the known protein structure (Figure 6), most of the changes found seem reasonable and suggestive, even though the chemical shift data cannot specify stereochemical details of the redox-dependent structure changes that occur. Takano and Dickerson (1981b) have discussed the changes they find in terms of possible causative stereochemical and/or electrostatic interactions.

Diamagnetic Origin of the Chemical Shift Changes. The chemical shift discrepancies observed cannot be attributed in the main to displacement of the affected protons in the paramagnetic field. Such an effect would not selectively shift the NH protons. Also, the analysis shows that the displacement in the paramagnetic shift field necessary to produce the chemical shift discrepancy observed for many of the protons, especially those in the 40s and 50s segments, is unrealistically large. Note that the *minimum* real space displacement necessary to produce the shifts observed (Table III) is given by $1.7\delta l_{crit}$.

It therefore appears that the chemical shift discrepancies found here must be predominantly diamagnetic in origin, caused ultimately by structural effects that include the segments listed in Table III. A major general role for ring current effects, due to changes in neighboring aromatic rings or the heme group itself, can be ruled out, since the *total* ring current shift effect felt by most of the protons listed in Table III is less than the chemical shift discrepancy observed (calculated by using a program provided by D. Case and P. E. Wright).

Absence of Structure Change. This work was done to search for redox-dependent structure change. In one sense, a large fraction of the amino acid residues in cytochrome c appear redox sensitive by some measure, including 19 residues found in both the NMR and X-ray investigations, 10 residues implicated only by NMR, 9 marked only in the X-ray work, and, in addition, the several heme-associated residues. However, the overall impression painted by the results is one of structural stability, i.e., the absence of conformational change. Protons at about 300 sites throughout the protein, other than those listed in Tables II and III, fail to show redox-dependent chemical shifts that pass the criterion set up here. When one or two protons in a given residue exhibit change and the others

do not, this suggests that the entire residue is not significantly displaced or its locale rearranged, but rather that chemical shifts can be quite sensitive to subtle structural effects, and especially so for peptide NH (Table II). It appears that the changes seen can be best visualized as slight readjustments to redox-induced strain, within a given structural free energy well, rather than as a directed transition into an alternative well.

What then is the basis for the physical–chemical differences seen between the reduced and oxidized proteins? According to linked function theory (Wyman, 1964), the fact that the cytochrome *c* protein favors the reduced form of its bound heme means that the heme binds more strongly to the protein in the reduced form and therefore makes reduced cytochrome *c* the more stable form. The higher structural free energy level of the oxidized protein reveals itself when structural stability is measured, e.g., in equilibrium denaturation experiments which measure overall stability and, at higher resolution, in the hydrogen-exchange rates of individual hydrogens, which depend upon local unfolding reactions (Englander & Kallenbach, 1984). The higher structural free energy of the oxidized protein will result in conformational change only if parts of the protein find a stable alternative folding that lowers their energy. The NMR results presented here and available X-ray diffraction results (Takano & Dickerson, 1981a,b; A. Berghius and G. D. Brayer, personal communication) indicate that this does not occur.

ACKNOWLEDGMENTS

Registry No. Cytochrome *c*, 9007-43-6; heme, 14875-96-8.

REFERENCES

Angstrom, J., Moore, G. R., & Williams, R. J. P. (1982) *Biochim. Biophys. Acta 703*, 87–94.

Arean, C. O., Moore, G. R., Williams, G., & Williams, R. J. P. (1988) *Eur. J. Biochem. 173*, 607–615.

Butt, W. D., & Keilin, D. (1962) *Proc. R. Soc. London, B 156*, 429–458.

Eden, D., Matthew, J. B., Rosa, J. J., & Richards, F. M. (1982) *Proc. Natl. Acad. Sci. U.S.A. 79*, 815–819.

Englander, S. W., & Kallenbach, N. R. (1984) *Q. Rev. Biophys. 16*, 521–655.

Feng, Y. (1989) Ph.D. Dissertation, University of Pennsylvania.

Feng, Y., Roder, H., Englander, S. W., Wand, A. J., & Di Stefano, D. L. (1989) *Biochemistry 28*, 195–203.

Feng, Y., Roder, H., & Englander, S. W. (1990) *Biophys. J. 57*, 15–22.

Horrocks, W. D., Jr., & Greenberg, S. (1973) *Biochim. Biophys. Acta 322*, 38–44.

Jardetzky, O., & Roberts, G. C. K. (1981) *N.M.R. in Molecular Biology*, Chapter 3, pp 69–83, Academic Press, New York.

Keller, R. M., & Wüthrich, K. (1972) *Biochim. Biophys. Acta 285*, 326–336.

Keller, R. M., & Wüthrich, K. (1978) *Biochem. Biophys. Res. Commun. 83*, 1132–1139.

Kharakoz, D. P., & Mkhitaryan, A. G. (1986) *Mol. Biol. 20*, 396–406.

Kurland, R. J., & McGarvey, B. R. J. (1970) *J. Magn. Reson. 2*, 286–301.

Labhardt, A., & Yuen, C. (1979) *Nature 227*, 150.

LaMar, G. N., & Walker, F. A. (1979) in *The Porphyrins* (Dolphin, D., Ed.) Vol. 4, pp 61–157, Academic Press, New York.

Lee, L., & Sykes, B. D. (1983) *Biochemistry 22*, 4363–4373.

Lee, L., Sykes, B. D., & Birnbaum, E. R. (1979) *FEBS Lett. 98*, 169–172.

Liu, G., Grygon, A., & Spiro, T. G. (1989) *Biochemistry 28*, 5046.

Mailer, C., & Taylor, C. P. S. (1972) *Can. J. Biochem. 85*, 1048–1055.

Moore, G. R., Robinson, M. N., Williams, G., & Williams, R. J. P. (1985) *J. Mol. Biol. 183*, 429–446.

Osheroff, N., Brautigan, D. L., & Margoliash, E. (1980) *Proc. Natl. Acad. Sci. U.S.A. 77*, 4439–4443.

Patel, D. J., & Canuel, L. L. (1976) *Proc. Natl. Acad. Sci. U.S.A. 73*, 1998.

Redfield, A. G., & Gupta, R. J. (1971) *Adv. Magn. Reson. 5*, 82–113.

Santos, H., & Turner, D. L. (1987) *FEBS Lett. 226*, 179–185.

Satterlee, J. D. (1986) *Annu. Rep. NMR Spectrosc. 17*, 79–178.

Senn, H., Keller, R. M., & Wüthrich, K. (1980) *Biochem. Biophys. Res. Commun. 92*, 1362–1369.

Senn, H., Guerlesquin, F., Bruschi, M., & Wüthrich, K. (1983) *Biochim. Biophys. Acta 748*, 194–204.

Shulman, R. G., Glarum, S. H., & Karplus, M. (1971) *J. Mol. Biol. 57*, 93–115.

Takano, T., & Dickerson, R. E. (1981a) *J. Mol. Biol. 153*, 79–94.

Takano, T., & Dickerson, R. E. (1981b) *J. Mol. Biol. 153*, 95–115.

Trewhella, J., Carlson, V., Curtis, E. H., & Heidorn, D. B. (1988) *Biochemistry 27*, 1121–1125.

Ulmer, D. D., & Kägi, J. H. (1968) *Biochemistry 7*, 2710–2717.

Wagner, G., Pardi, A., & Wüthrich (1983) *J. Am. Chem. Soc. 105*, 5948–5949.

Wand, A. J., Roder, H., & Englander, S. W. (1986) *Biochemistry 25*, 1107–1114.

Wand, A. J., Di Stefano, D. L., Feng, Y., Roder, H., & Englander, S. W. (1989) *Biochemistry 28*, 186–194.

Williams, G., Moore, G. R., Porteous, R., Robinson, M. N., & Williams, R. J. P. (1985a) *J. Mol. Biol. 183*, 409–428.

Williams, G., Clayden, N. J., Moore, G. R., & Williams, R. J. P. (1985b) *J. Mol. Biol. 183*, 447–460.

Wüthrich, K. (1976) *NMR in Biological Research: Peptides and Proteins*, North-Holland/Elsevier, Amsterdam, New York.

Wüthrich, K., & Baumann, R. (1974) *Helv. Chim. Acta 57*, 336.

Wüthrich, W., Shulman, R. G., Wyluda, B. J., & Caughey, W. S. (1969) *Proc. Natl. Acad. Sci. U.S.A. 62*, 636–649.

Wyman, J. J. (1964) *Adv. Protein Chem. 19*, 223–286.